Biodegradable fishing gears: A potential solution to ghost fishing and marine plastic pollution

Waranya Wataniyakun [a,*], Maelenn Le Gall [b], Maria El Rakwe [b], Christian W. Karl [c], Roger B Larsen [a]

[a] UiT The Arctic University of Norway, N-9037 Tromsø, Norway
[b] Ifremer, RDT Research and Technological Development Unit, F-29280 Plouzané, France
[c] SINTEF Industry, Polymer and Composite Materials, N-0373 Oslo, Norway

ARTICLE INFO

ABSTRACT

Fishing gears are conventionally made from non-biodegradable materials including polyamide (PA). When lost in the ocean, these gears have long-lasting impacts, including marine littering, microplastics production, leaching of chemicals, and an extended period of ghost fishing due to its durability. The use of biodegradable *co*-polyester material such as polybutylene succinate *co*-adipate-co-terephthalate (PBSAT) and polybutylene succinate-*co*-butylene adipate (PBSA) as fishing gear materials have been considered as a potential solution to reduce the associated impact. Ocean is a complex environment in which multiple degradation paths can occur for plastic materials, and decoupling of factors could aid in understanding the impact of each potential factor. In this study, the focus is on the impact of pure water hydrolysis phenomena on biodegradable *co*-polyester PBSAT and PBSA in comparison to PA monofilaments through accelerated aging at 40 °C, 60 °C, 70 °C and 80 °C. As a single factor accelerated aging process, the prediction of loss of mechanical strength over time was possible at other temperatures namely 2 °C, 10 °C, 15 °C, 20 °C and 30 °C. Different end-of-life criteria were used. This study concluded that solely through pure hydrolysis, a drastic reduction of the time to reach end-of-life criteria was observed by using biodegradable monofilaments instead of PA, but still longer than the expected service time. For example, at 2 °C, it would take approximately 10 years, 20 years and 1000 years for PBSAT, PBSA and PA to have lost 50 % of their initial stress at break respectively.

1. Introduction

Regardless of the location of production, usage or disposal, the global oceans seems to be the final destination for the large part of plastic wastes produced on Earth (Wang et al., 2016). Plastics is ubiquitous to our daily life since its mass production in the 1940s, and has become one of the most indispensable materials to date across all industry, including fisheries (Bergmann et al., 2022; Geyer et al., 2017; Jambeck et al., 2015). As a marine-based operation, fisheries activity represent one of the most direct plastic-ocean contacts, and present a direct pathway of plastics entering the ocean as waste without any treatment process in between (Lusher et al., 2017).

Abandoned, lost or otherwise discarded fishing gears (ALDFG) are fishing gears that enter the ocean both intentionally and unintentionally after or during their deployment (Macfadyen et al., 2009). Entanglement and ingestion of organisms were amongst the first visible impacts of

plastic pollution that removed the first layer of the rose-tinted view of plastics as early as barely two decades after industrialisation of plastics (Laist, 1987; Thompson et al., 2009). This impact is further intensified by the designed-to-capture nature of ALDFG, where the impact is plausibly more detrimental than other plastic wastes that enter the ocean when it comes to marine organisms' welfare (Wilcox et al., 2016).

In addition to entanglement of species resulting in mortalities, ALDFG could result in ghost fishing phenomena. The term ghost fishing, first documented in 1978 and later defined in 1985 by FAO, refers to the ability of ALDFG to continue catching and causing mortality to marine organisms in the absence of fishers' control (Brown et al., 2005; Laist, 1997; Macfadyen et al., 2009; Smolowitz, 1978). ALDFG is also estimated to contribute up to one-fifth of the total ocean plastics (Morales-caselles et al., 2021). In a recent study in collaboration with the Norwegian Directorate of Fisheries' annual lost fishing gear retrieval operations, ghost fishing in the near coast area of Finnmark in northern
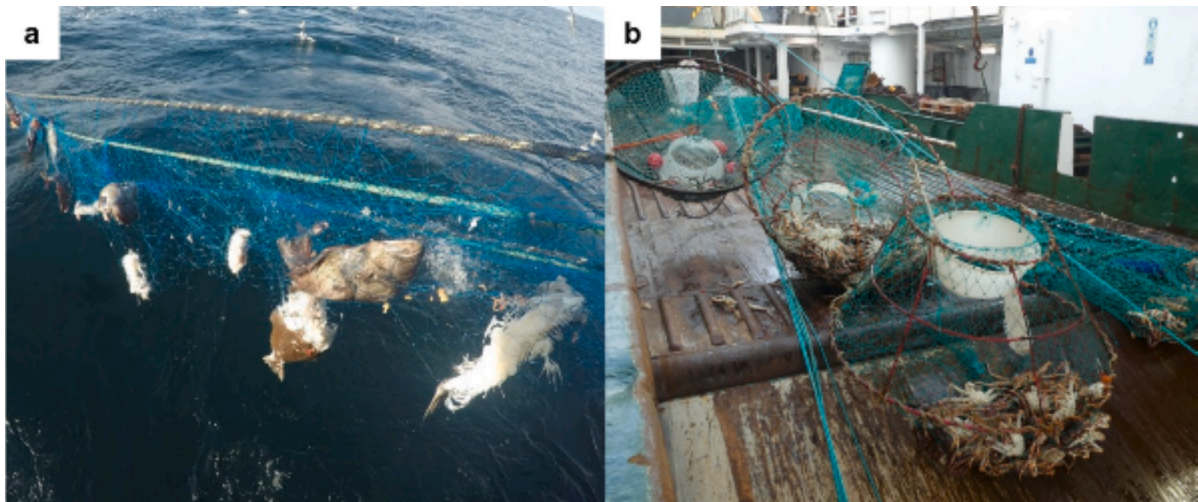
Fig. 1. Images from October 2024 during the annual Norwegian ALDFG clean-up operation organized by the Directorate of Fisheries: (a) a gillnet used in the Norwegian deep-water fishery for Greenland halibut (*Reinhardtius hippoglossoides*) recovered. Photo by Gjermund Langedal, the Directorate of Fisheries and (b) King crab (*Paralithodes camtschaticus*) pots retrieved at Nordkappbanken, Northern Norway (71° 12 N - 25° 59 E). Photo by R.B. Larsen, UiT The Arctic University of Norway.

Norway was observed in three-quarters of the retrieved gillnets and about two thirds in king crab pots (Vodopia et al., 2024). Images of some ghost fishing observed from this retrieval operations are shown in Fig. 1. The number of gillnets retrieved during the annual retrieval operations by the Norwegian directorate of fisheries increased from 935 pieces in 2014 to 1339 in 2023 (Norwegian Directorate of Fisheries, 2023).

Ghost fishing is particularly dire in passive fishing methods where the capture mechanism is reliant on movement of desired species. (Gilman et al., 2016; IWC, 2013; World Animal Protection International, 2014). It affects both targeted and untargeted species, and do not stay in one position. It can therefore affect many species across a large area and depth (Gilman et al., 2016; Good et al., 2010). Since the fishing gears are designed to capture a particular species or sizes, some species may be more at risks than others. (Brown et al., 2005; Link et al., 2019; World Animal Protection International, 2014).

In addition to main target species that are exposed to ghost fishing, a secondary process is prone to take place in several fisheries where different scavenger species are approaching the gear due to already ghost fished animals acting as "bait" in such gears. This results in a long lasting re-baiting and capture process until the fishing gear can no longer fish due to excessive biofouling or degradation to a state where all animals can escape. Injury and death from ghost fishing can happen in various ways - suffocation, drowning, starvation, or the inability to escape predators (Hammer et al., 2012; Rhodes, 2018).

Alongside extended period of ghost fishing due to the persistent presence of conventional ALDFG, other associated problems would also affect the environment for longer duration. These problems include microplastics formation, leaching of harmful substances such as additives and chemicals from ALDFG, and for ALDFG, whether in its intact form or as broken down microplastics, to behave as a vector for these chemicals. Microplastics could behave as a vector to introduce these chemicals into organisms, while ALDFG could transport these chemicals to other areas of the ocean due to tidal movements (Fauser et al., 2022; Hahladakis et al., 2018; Hermabessiere et al., 2017; Jang et al., 2024; Kiessling et al., 2015; Koelmans et al., 2016).

Fishing gears, buoys and lines are manufactured almost exclusively of plastics. Commonly used polymers and their associated gears are nylon or polyamide (PA), polyester (PES), polyethylene (PE) and polypropylene (PP) as the principal building blocks of modern fishing gears (Deshpande et al., 2020). Despite often having as short service time as 18 to 24 months, these polymers could last up to centuries when lost in the ocean (Barnes et al., 2009; Deshpande et al., 2020; Vodopia et al.,

2024). Over time, this could result in the spread of waste in coastal areas and the open sea, with the greatest accumulation occurring on the seabed (Galgani et al., 2015).

Degradation of plastics is largely divided into abiotic and biotic degradation and highly depends on several factors including but not limited to exposure to light, temperature, pH, wave actions and presence of microorganisms (Lucas et al., 2008; Min et al., 2020). Abiotic degradation can further be divided into two pathways – physical and chemical degradation, with the two main chemical degradation being oxidation and hydrolysis (Lucas et al., 2008). Besides the external factors, presence of functional groups within polymers such as esters, amides and carbonates that are susceptible to hydrolysis play an important role in the degradation process of a material (Gewert et al., 2015; Min et al., 2020).

According to a study done by Krause et al. (2020), PP and PE plastic debris that presumably entered the ocean more than two decades ago showed no significant sign of degradation (Krause et al., 2020). Welden and Cowie (2017), examined the degradation of ropes in marine environment, 10 m below the surface with temperature ranging from 5.7 °C to 17.9 °C throughout the 12-months period and observed an average mass loss of 0.39 %, 1.02 % and 0.45 % per month in PP, nylon and PE respectively (Welden and Cowie, 2017). However, for most ALDFG, they would be submerged at a much deeper level than 10 m with consequently lower temperature and limited to no light exposure. Based on the rankings from Min et al. in 2020, it was also stated that nylon degrades slower than polyester (Min et al., 2020).

Since many fishing gears, for example gillnets, are being used for relatively short period, use of biodegradable material are discussed as a potential solution to issues arising from ALDFG under uncontrollable circumstances (Barnes et al., 2009; Grimaldo et al., 2023; Le Gué et al., 2024). With the lack of light and therefore UV exposure at the seafloor, hydrolytic degradation would play a key role in degradation of these ALDFG. Given that the ester bond is highly susceptible to hydrolysis in comparison to PA, PES, PE or PP, a *co*-polyester biodegradable material such as polybutylene succinate *co*-adipate-co-terephthalate (PBSAT) and polybutylene succinate-*co*-butylene adipate (PBSA) might be a potential solution to reducing ghost fishing impact and marine plastic pollution (Gewert et al., 2015; Min et al., 2020; Summers and Rabinovitch, 1999).

This study aims to compare the degradation of biodegradable PBSAT and PBSA monofilaments with traditional PA monofilaments through accelerated aging experiments, in order to describe the first step in predicting their expected lifespan in marine environments. Degradation
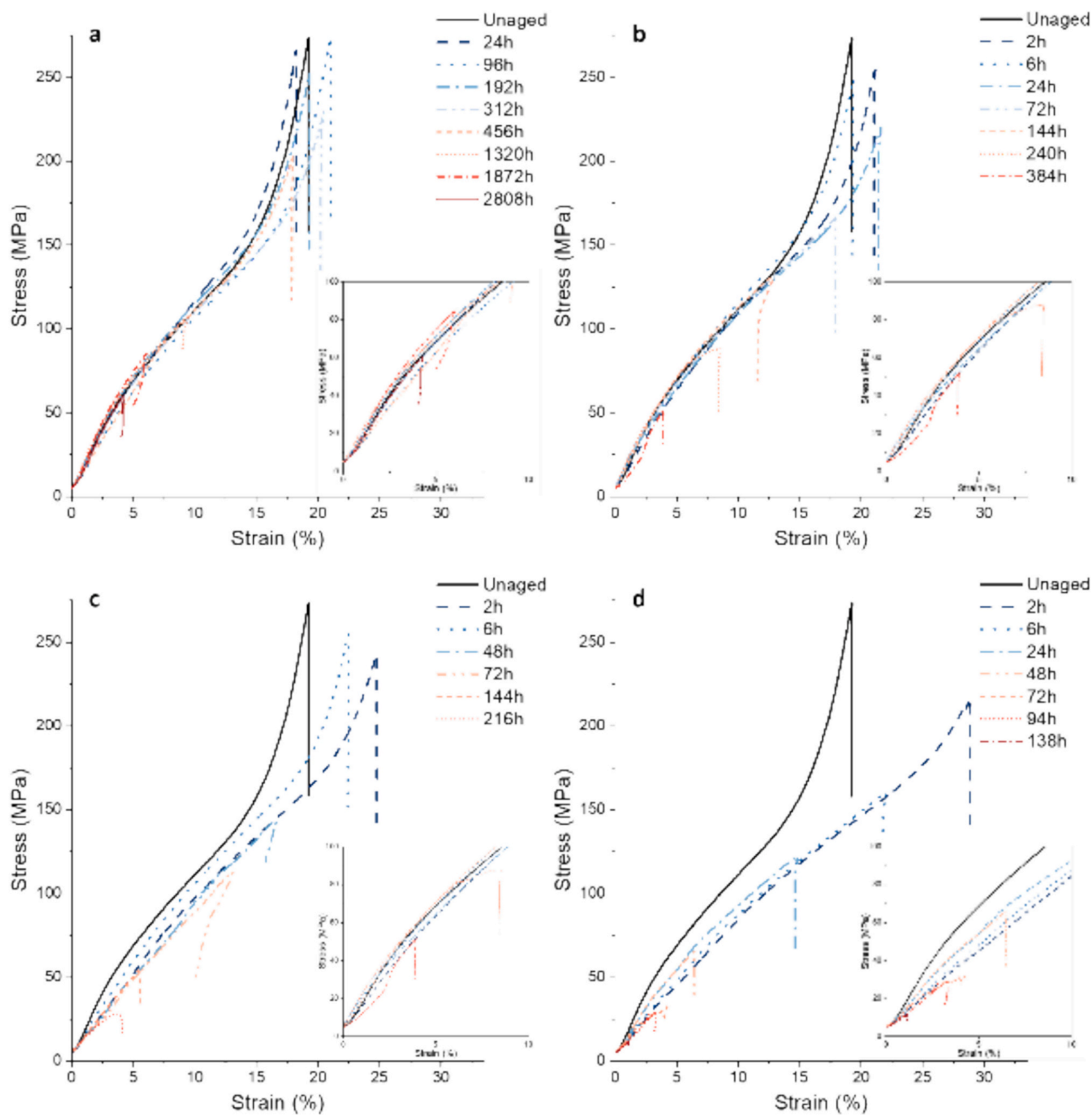
Fig. 2. Stress-strain curves of PBSAT along aging in deionised water at (a) 40 °C, (b) 60 °C, (c) 70 °C and (d) 80 °C with a zoomed-in inset for up to 10 % strain.
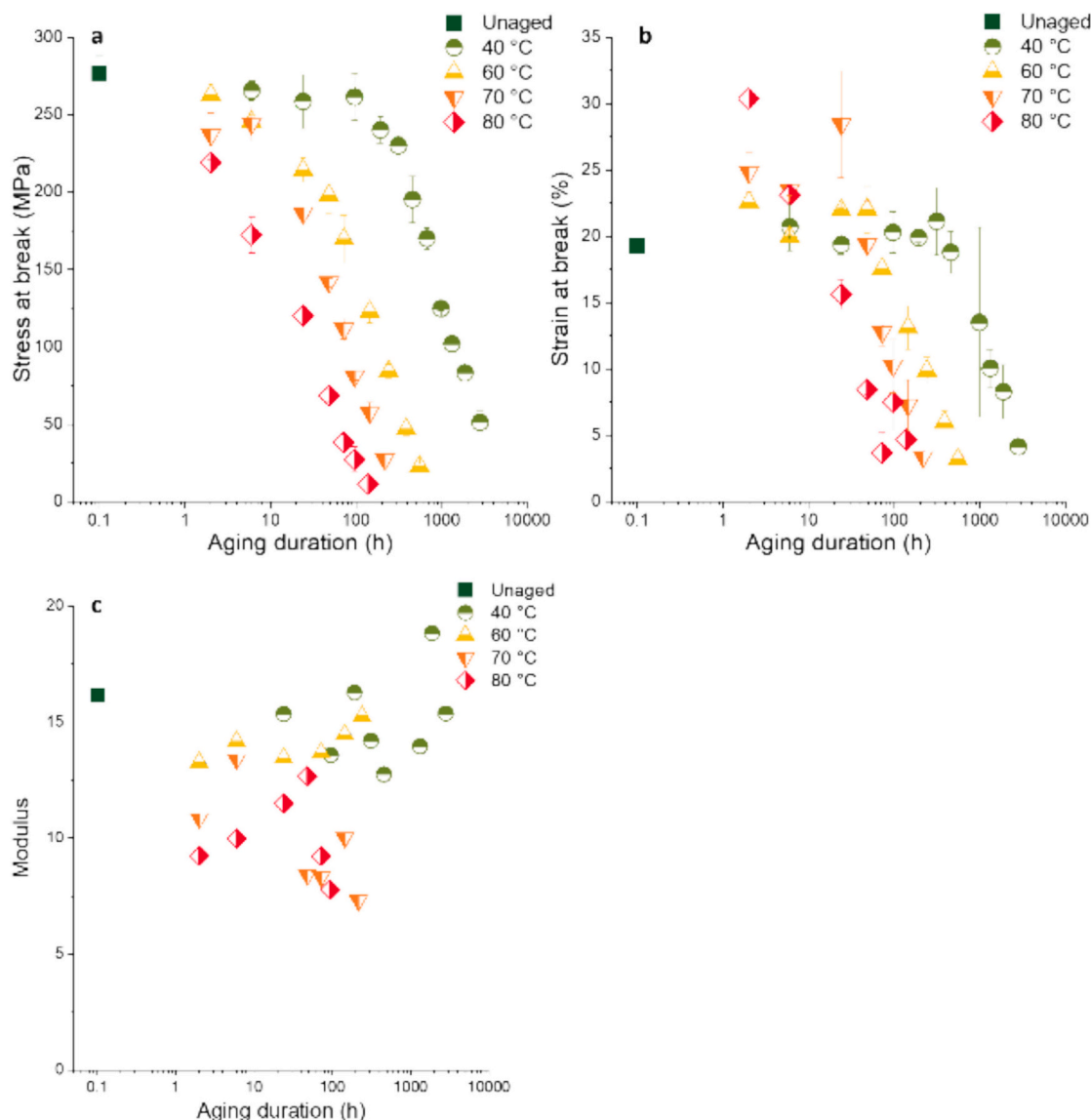
Fig. 3. Average (a) stress at break, (b) strain at break and (c) modulus in function of the aging duration for PBSAT aged at 40 °C, 60 °C, 70 °C and 80 °C.

factors, such as UV exposure and microorganisms, vary depending on ocean location and depth. While biodegradable materials are vulnerable to microbial degradation, this is not the case for PA, at least during the early stages of aging. However, all three materials are affected by hydrolysis. To ensure a fair comparison between biodegradable and traditional materials, while eliminating location-specific variables, this study focuses on a universal degradation factor: the presence of water. Aging experiments are conducted in pure water rather than seawater, representing the worst-case scenario for the new materials, where biodegradation may not occur.

Accelerated aging experiments in laboratory settings are a common way to examine reactions in an accelerated manner to shorten the time required for reactions that would otherwise take far too long in environmental conditions. For this study, hydrolysis of materials is accelerated by elevating the submersion temperatures. From experimental values, a model using Arrhenius approach would be performed to predict the time to reach end-of-life of the material, which could be used to estimate the time required for the materials to lose the mechanical properties in the environment. To our knowledge, there has been no studies that link pure water hydrolysis accelerated aging with regards to ghost fishing impact.

2. Materials and methods

2.1. Material

The three materials used in this experiment are PA (LG Chem Ltd., South Korea), PBSAT (LG Chem Ltd., South Korea) and PBSA (LG Chem Ltd., South Korea). Samples are monofilaments produced and developed for fishing gear applications with an average diameter of 0.57 mm for PA and 0.60 mm for both PBSAT and PBSA. These monofilaments were cut into pieces of between 8 and 10 cm prior to the experiment. The differing length is due to the different material availability. PA is transparent light blue in colour, PBSAT is transparent green in colour and PBSA is a slightly translucent white.

2.2. Aging method

Accelerated pure hydrolysis aging was conducted in deionised (DI) water tanks at IFREMER Centre Bretagne at four different temperatures namely 40 °C, 60 °C, 70 °C and 80 °C. These relatively high temperatures were selected to ensure an accelerated aging process. DI water in the tanks was in constant circulation. Between 50 and 70 samples of each material were placed into a container with holes to ensure constant
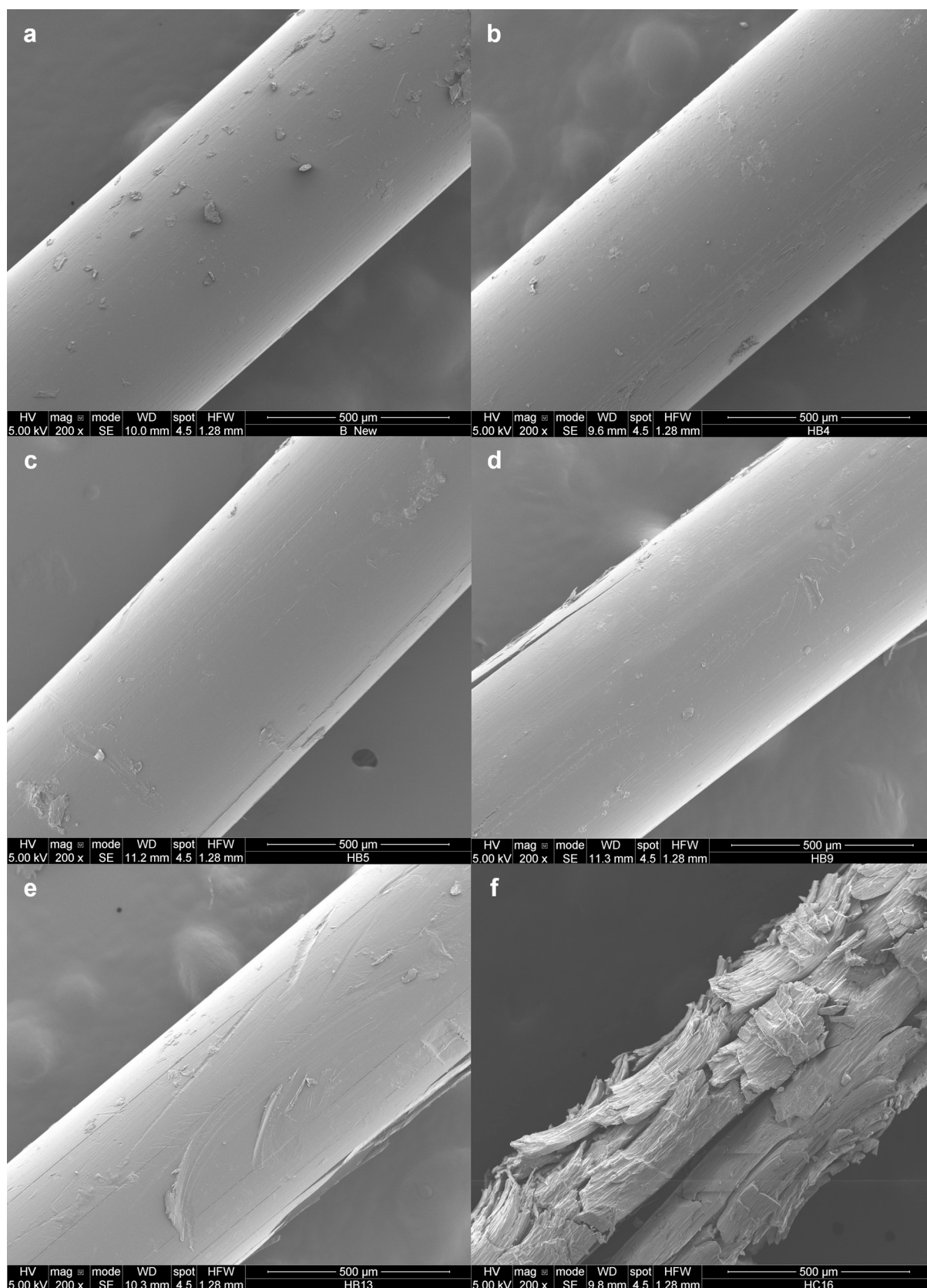
Fig. 4. SEM pictures of (a) unaged PBSAT, (b) aged PBSAT at 40 °C for 672 h, (c) aged PBSAT at 70 °C for 48 h, (d) aged PBSAT at 60 °C for 240 h, (e) aged PBSAT at 60 °C for 384 h and (f) aged PBSAT at 60 °C for 552 h.
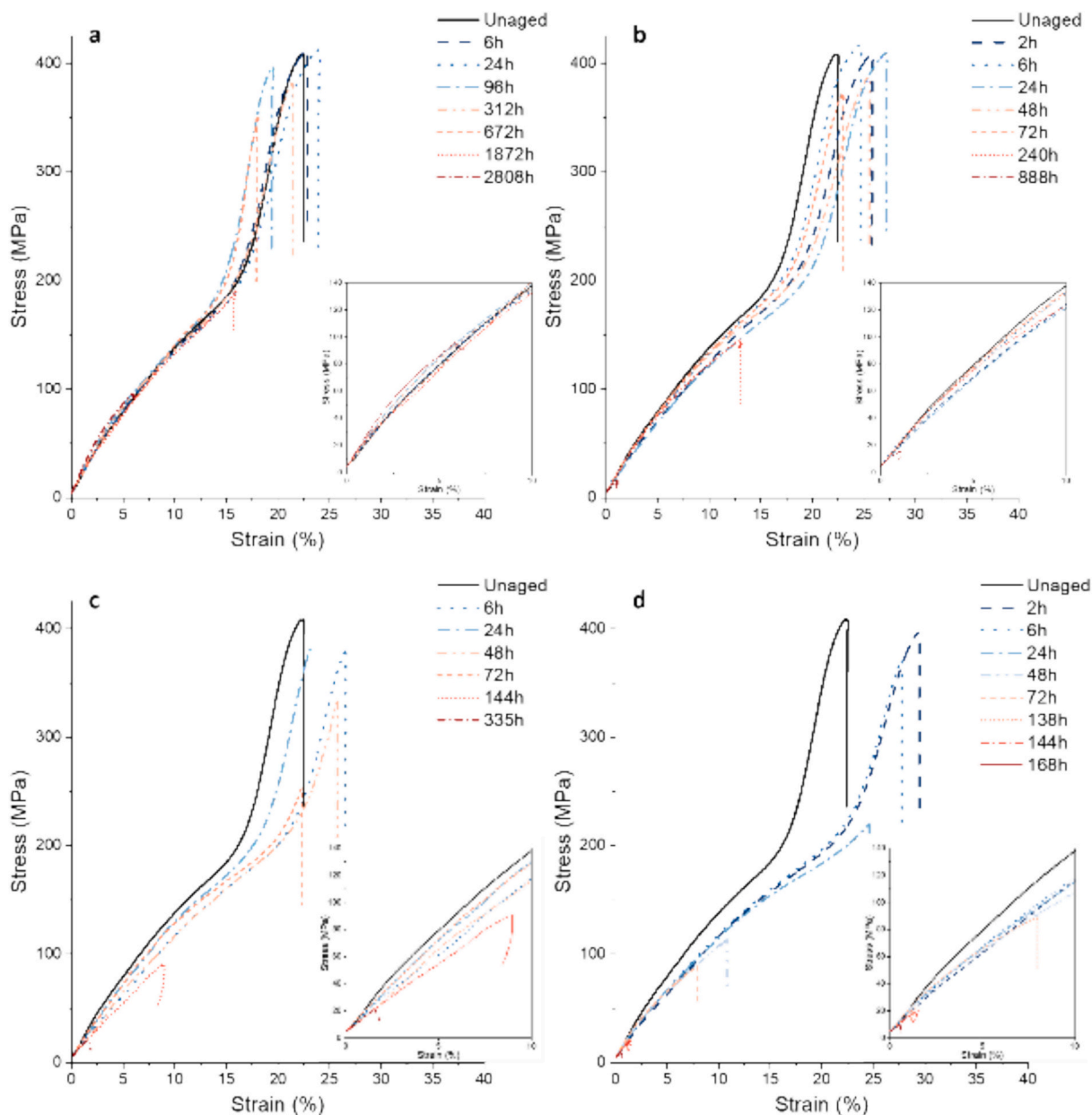
Fig. 5. Stress-strain curves of PBSA along aging in deionised water at (a) 40 °C, (b) 60 °C, (c) 70 °C and (d) 80 °C with a zoomed-in inset for up to 10 % strain.

water renewal. The sampling duration varied from temperature to another, starting as early as 2 h and up to over 2000 h until one of the materials become brittle. The sampling time points are available throughout the results section.

At each sampling point, four pieces of samples were taken out and placed in a controlled desiccator cabinet with relative humidity of 8.7 % at 21.5 °C for at least 24 h prior to further tests.

2.3. Mechanical testing

For each material, at each aging temperature and time point, a tensile strength test was carried out on the samples. Due to the length constraint of the sample, the monofilaments were clamped at two ends. The tensile strength test was done uniaxially with Instron 5966 (Instron®, United States of America) with video extensometer to track the strain. The tensile strength test was performed with 500 N load cell with displacement speed of 10 mm/min. All measurements were done in at least triplicates. The modulus was calculated between strain 0.85 % to

1.6 % for PBSAT and between 0.6 % and 1.7 % for PBSA. All tests were carried out in a room with constant controlled temperature of 21 °C ± 2 °C and 50 % ± 10 % relative humidity.

2.4. Scanning electron microscopy (SEM)

Surface morphology of samples was analysed using a scanning electron microscope (SEM) (FEI Quanta 200, Thermo Fisher Scientific, United States of America). Each sample was completely dried before being coated with gold particle to reduce static prior to the analysis.

2.5. Statistical analysis

Statistical analysis was performed using SPSS (IBM, United States of America) to obtain the mean and standard deviation. Data was also analysed with one-way ANOVA test with Duncan post-hoc to determine statistical significance with *p*-value of 0.05. All figures were plotted using OriginPro 2019b and OriginPro 2024 (OriginLab, United States of
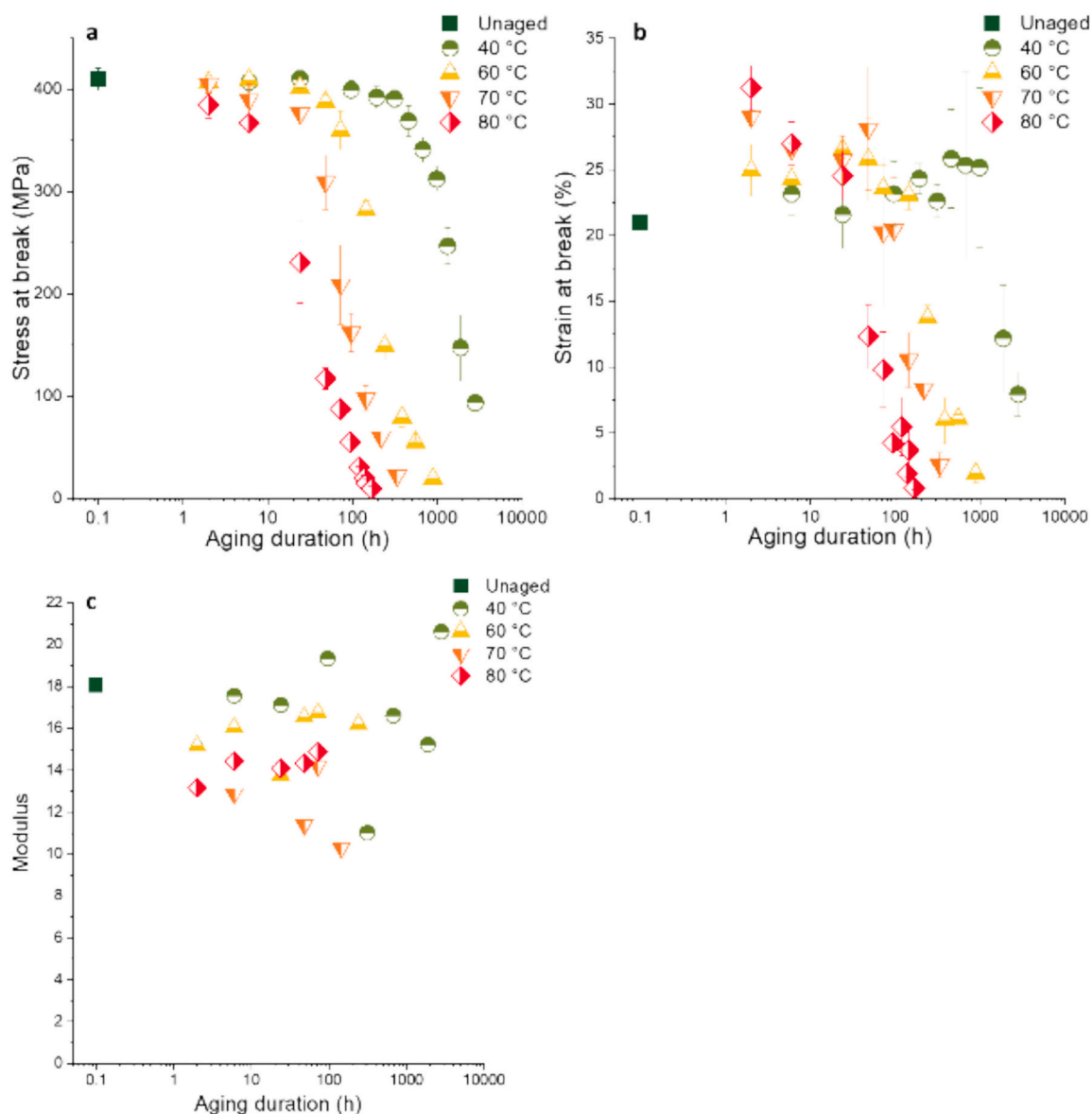
Fig. 6. Average (a) stress at break, (b) strain at break and (c) modulus in function of the aging duration for PBSA aged at 40 °C, 60 °C, 70 °C and 80 °C.

America).

3. Results

This section aims to present experimental data obtained with the three materials considered in this study, especially changes in mechanical behaviour with aging.

3.1. PBSAT

The focus in this section is on the mechanical behaviour of PBSAT and its changes of properties during aging. Fig. 2 shows the stress-strain curve of PBSAT during aging at 40 °C, 60 °C, 70 °C and 80 °C for various aging time.

The unaged PBSAT sample, presented as solid line in Fig. 2a to Fig. 2d, exhibited a typical behaviour for monofilament in polymer with a linear section (from 0 to 1.6 %) where it was possible to calculate a modulus that describes the stiffness of the material. Then a non-linear behaviour occurred beyond this region due to the specific changes to the microstructure of semi crystalline polymer. The sample finally broke when it could not be further stretched. Both average stress and strain at

break could be calculated based on the triplicates. Prior to aging, unaged PBSAT monofilament had an average stress at break of 276.8 ± 11.1 MPa and strain at break of 19.3 ± 2.2 %.

During aging, large changes in mechanical behaviour occurred. A slight increase in strain at break was observed throughout the aging temperature. For example, at 60 °C a slight increase in elongation at break for the early stage of aging where the strain at break increases from 19.3 ± 2.2 % to 22.0 ± 1.8 % after 48 h of immersion was observed. For longer aging duration, a large and gradual decrease in both stress and strain at break occurs, due to an embrittlement of the material induced by the hydrolysis of the polymer. The same behaviour was observed for all aging temperature considered here but an increase in degradation rate was observed as can be seen in Fig. 3.

Fig. 3 shows the average stress at break, average strain at break and modulus with respect to aging duration across different temperatures. The aging time required to reduce the stress at break to less than half of unaged material was 24 h, 48 h, 144 h and 984 h for 80 °C, 70 °C, 60 °C and 40 °C respectively. Overall, the average stress at break declined with aging time in all temperatures, with decreasing rates as aging temperature decreases. Tables S1.1 to S1.4 summarizing statistical differences is available in section S1 of the supplementary document.
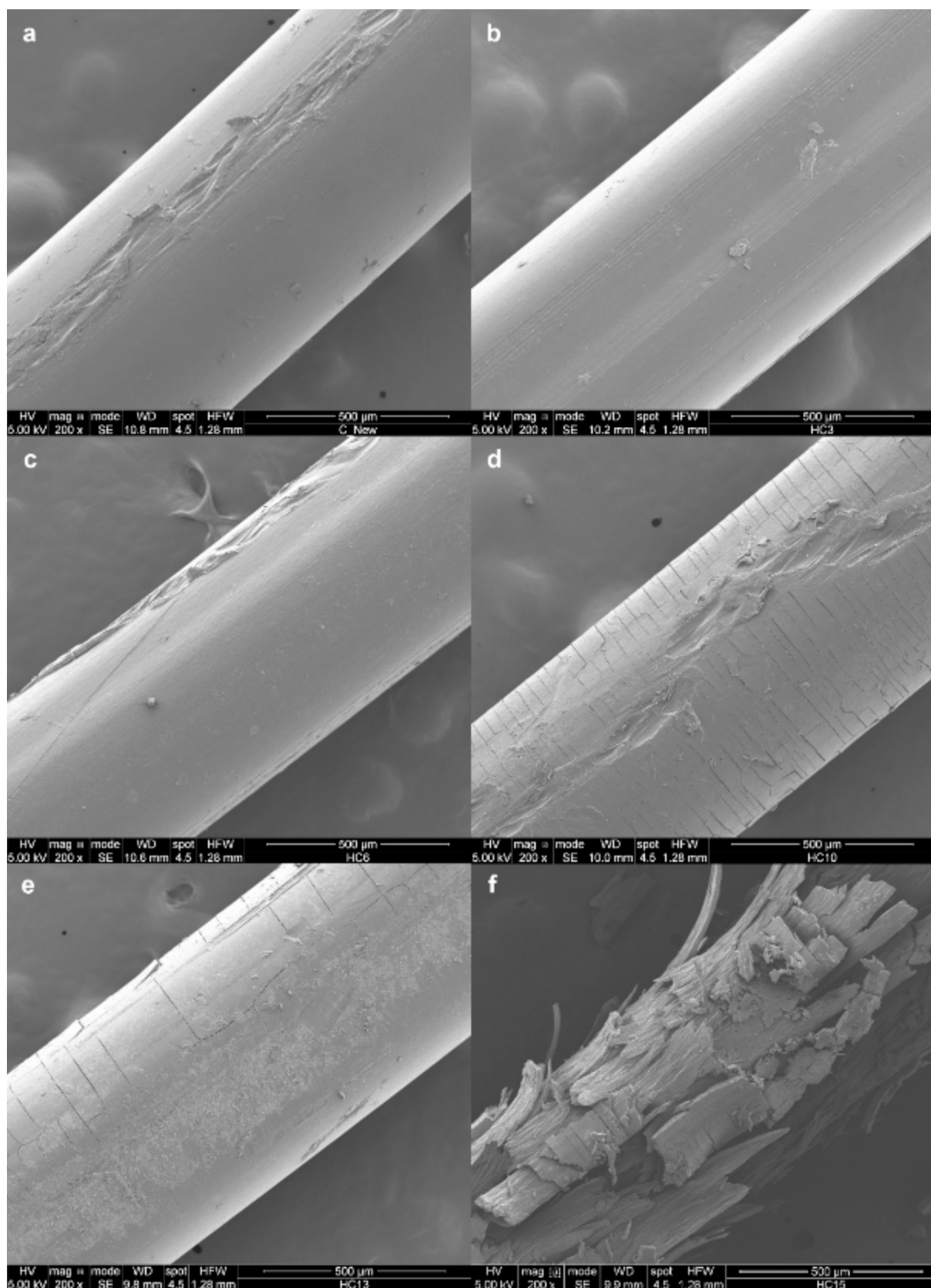
Fig. 7. SEM image of (a) unaged, (b) aged PBSA at 70 °C for 48 h, (c) aged PBSA at 80 °C 24 h, (d) for aged PBSA at 80 °C for 48 h, (e) aged PBSA at 70 °C for 216 h and (f) aged PBSA at 70 °C for 335 h.
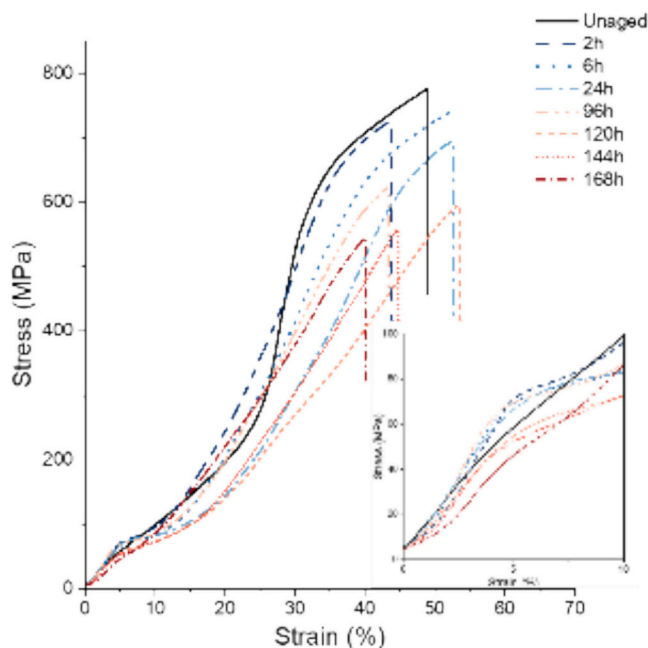
Fig. 8. Stress-strain curves of PA along aging at 80 °C with a zoomed-in inset for up to 10 % strain.

The modulus of unaged PBSAT was 16.2 MPa. Plot showing modulus values across different aging conditions are shown in Fig. 3c. There was no clear trend observed in the modulus of the strain-stress curve.

The surface morphology of monofilaments was observed under scanning electron microscope (SEM). Unaged PBSAT had a smooth surface with some axial crack, likely from the production process shown in Fig. 4a. As seen in Fig. 4b and Fig. 4c, there are barely any visible changes to the surface morphology despite being at 61.4 % and 51.1 % of the initial stress with stress at break of 170.1 ± 6.9 MPa and 141.7 ± 3.0 MPa respectively. A deeper crack was seen along the fibre in Fig. 4d, but no other visible change was observed. The average stress at break for Fig. 4d's aging condition was at 84.2 ± 4.5 MPa, approximately 30 % of the unaged material's stress at break. With barely 16.9 % of the initial stress at 46.8 ± 4.4 MPa, surface morphology of PBSAT still showed very little change except for some peeling on the surface as shown in Fig. 4e. SEM of extremely aged sample as seen in Fig. 4f showed fragmentation of monofilaments into microfibres, with average stress at break of 22.9 ± 1.7 MPa or equivalent to <10 % of the initial stress at break. With a consecutively lower stress at break shown from Fig. 4b to Fig. 4f, there was no gradual change in the physical appearance of the monofilaments together with the reduction in material's mechanical properties, but rather an abrupt change in appearance between Fig. 4e and Fig. 4f, which were only approximately 8 % difference in comparison to the initial stress at break. There was no visible difference between Fig. 4a and Fig. 4e despite having an almost 85 % drop in stress at break. No change in diameter of the monofilament was observed through aging even in the extreme cases.

3.2. PBSA

The mechanical behaviour of PBSA and its changes of properties during aging is discussed here. Fig. 5 shows the stress-strain curve of PBSA during aging at 40 °C, 60 °C, 70 °C and 80 °C for various aging time, with unaged material represented in solid black line.

The stress-strain curves show a typical behaviour for monofilament in polymer with a linear section (from 0 to 1.7 %) where it was possible to calculate a modulus that described the stiffness of the material. The shape differs slightly from curves seen in Fig. 2. A non-linear region corresponded to behaviour that occurs due to the specific microstructure

of semi crystalline polymer. The sample eventually broke when it could elongate no further. Both average stress and strain at break could be calculated based on the triplicates. Unaged PBSA monofilament had an average stress at break of 410.0 ± 11.0 MPa and strain at break of 21.0 ± 2.4 %.

Fig. 6 shows the average stress at break, average strain at break and modulus with respect to aging duration across different temperatures. There is a decline in the stress at break across all temperature, with increasing time required until all the mechanical strength is lost as aging temperature decreases. In general, there were statistically significant differences across most time points in all aging temperatures. The aging time for the stress at break to be reduced to half was 48 h, 72 h, 240 h and 1872 h for aging temperatures 80 °C, 70 °C, 60 °C and 40 °C respectively. Tables S2.1 to S2.4 summarizing statistical differences is available in section S2 of the supplementary document.

Aging leads to changes in mechanical behaviour. Just like what was observed in PBSAT, the average strain at break increased in early-stage aging across all temperatures, followed by a drastic reduction of strain and stress at break.

The modulus of PBSA was calculated between 0.6 % to 1.7 % of the strain. Similar to that observed in PBSAT, there were no clear trend in the PBSA modulus. The modulus of the pristine material was 18.1 MPa. Modulus from aged materials fluctuated from 10.3 to 20.6 MPa, with the lowest modulus calculated in monofilaments aged at 80 °C and increased with decreasing aging temperature. The largest modulus calculated was in monofilaments aged at 40 °C.

The SEM images of PBSA surfaces are shown in Fig. 7.

Unaged PBSA exhibited a crack along the axis which resulted possibly from the extrusion manufacturing process in Fig. 7a. Fig. 7b and Fig. 7c with the average stress at break of 309.5 ± 26.8 MPa and 231.0 ± 40.1 MPa, approximately 75 % and 56 % of the initial stress at break, there were no other visible changes observed. Fig. 7d and Fig. 7e shows cracks on the surface of PBSA. The stress at break of Fig. 7d and Fig. 7e was 117.3 ± 10.3 MPa and 60.0 ± 1.8 MPa, or equivalent to approximately 28 % and 14 % of the initial stress at break. The aged PBSA at 70 °C for 335 h showed peeling along the monofilaments and deep cracks within the monofilament as seen in Fig. 7f. The average stress at break was 22.5 ± 4.6 MPa, just slightly above 5 % of the initial stress at break. There was no change in the diameter of the monofilaments, even when the monofilaments were extremely aged. Physical aging signs on the surface were not gradual, and only started first appearing after losing almost two-thirds of the initial stress at break.

3.3. PA

Aging of PA was also done at 40 °C, 60 °C, 70 °C and 80 °C. Only the resulting stress-strain curve of aging at 80 °C is displayed in Fig. 8 as there were no significant changes to the mechanical properties of PA aged at the other temperatures. For this reason, plots of average stress at break, strain at break, and modulus of PA are not displayed in this study as there were no comparison possible between all the aging temperatures. There is a decrease in the stress at break and strain over 168 h of aging at 80 °C as seen in Fig. 8. However, the decrease was not as drastic as observed in PBSAT and PBSA.

Unlike PBSAT and PBSA which became completely fragile after a shorter time, the average stress of PA only dropped approximately <30 % from 731.4 ± 31.2 MPa to 520.3 ± 25.2 MPa. There was no significant difference ($p > 0.05$) in the strain at break in all the aged timepoints in comparison to each other. They were all significantly higher than the pristine sample. Table S3.1 summarizing statistical differences is available in section S3 of the supplementary document.

The results for PBSAT and PBSA showed clear signs of degradation through hydrolysis. While not to the same extent, this was also observed in PA. Since all other aging conditions were identical, the changes observed in this section must be due to intrinsic properties of the material in response to pure water hydrolysis.
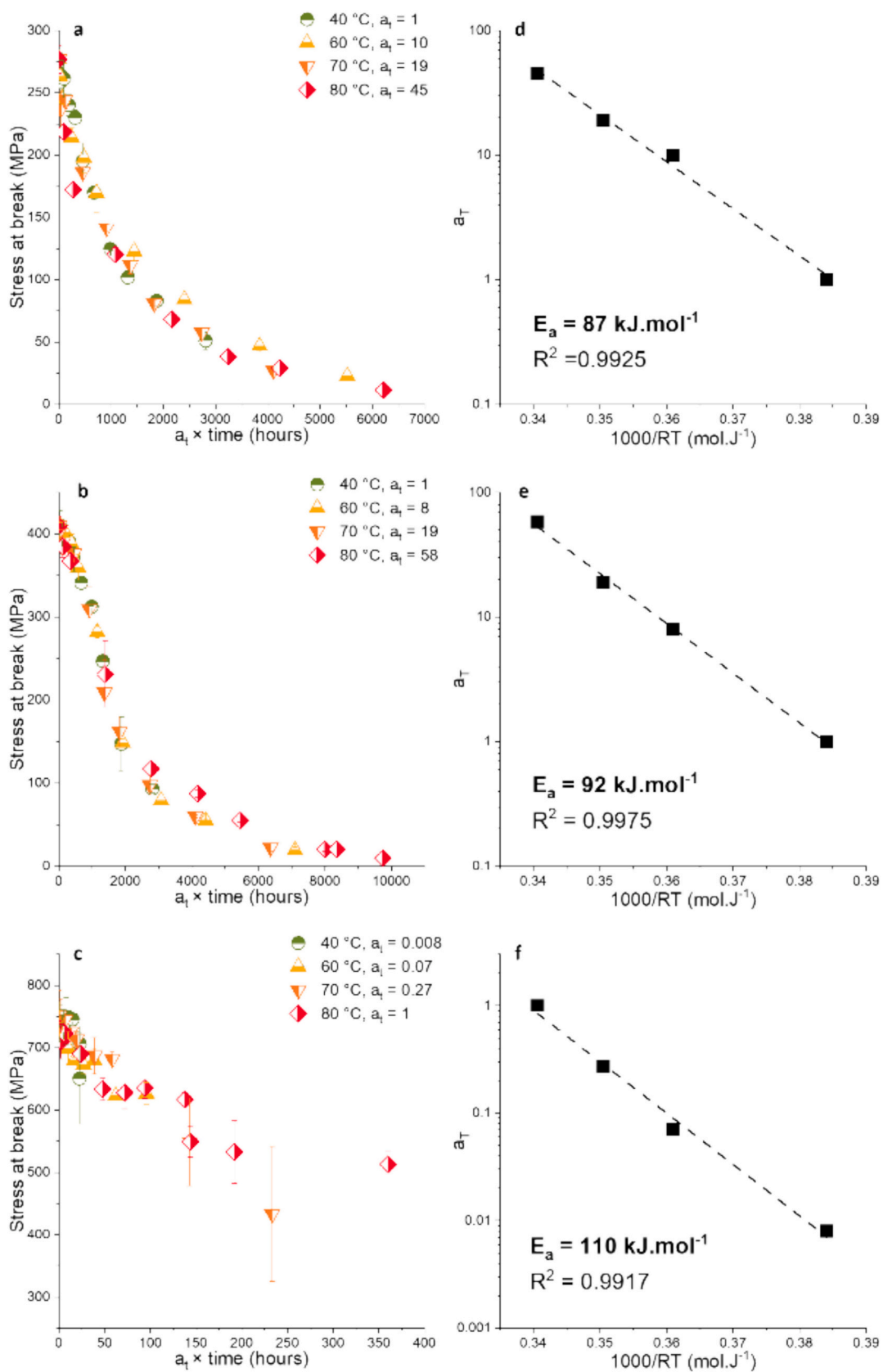
Fig. 9. Superposition time/temperature mastercurve of (a) PBSAT, (b) PBSA, and (c) PA, and shifting factor a_T in function of the temperature for the (d) PBSAT, (e) PBSA, and (f) PA.

Table 1

Shifting factor and activation energy.

Material	Initial stress at break (MPa)	Aging temperature (°C)	Shifting factor, a_T	Activation energy, E_a (kJ. mol^{-1})
PBSAT	276.8 ± 11.1	40	1	87
		60	10	
		70	19	
		80	45	
PBSA	410.0 ± 11.0	40	1	93
		60	8	
		70	19	
		80	58	
PA	731.4 ± 31.2	40	0.008	110
		60	0.07	
		70	0.27	
		80	1	

4. Discussion

In the previous section, the results had shown a clear reduction in average stress at break across all temperatures for the three materials. The materials were immersed in deionised water, an abiotic environment. Moreover, as the monofilaments are thin, the water diffusion happened quickly. Given that this was a reaction with one single mechanism namely pure water hydrolysis, the use of Arrhenius equation is employed for further discussion. In this section, the evaluation on the possibility of using Arrhenius approach to describe the degradation of the three materials and potentially predict their behaviour at lower temperatures was carried out.

4.1. Description of the mechanical consequences of the degradation

Accelerated aging test is an essential tool used to observe and understand the degradation behaviour within a study time frame. Temperature is often used as the accelerated factor, taking care of the thermal properties of the studied material. Arrhenius has defined an empirical equation giving the dependency of the rate of a chemical reaction with the temperature. This approach is based on single factor degradation mechanism, and therefore can be applied in our study case. The Arrhenius approach is described in Eq. 1,

$$a_T = a_0 e^{\left(-\frac{E_a}{RT}\right)} \tag{1}$$

where a_T is the rate of the reaction at a certain temperature, E_a the activation energy, R the universal gas constant and T the absolute temperature in K.

Following Arrhenius approach, the changes of properties observed at different times for the different aging temperatures should follow the same trend. It was therefore possible to superpose the change of property curves using a_T as a shifting factor, doing a so-called time/temperature superposition. For this study, as the stress at break was changing for all three materials during the aging, this mechanical property was therefore selected for performing superposition. For each material a mastercurve was obtained as shown in Fig. 9. The shifting factors were adjusted with reference to aging conditions at 40 °C for PBSAT and PBSA and 80 °C for PA, and can be found in the legend of the graphics presented in Fig. 9 and Table 1.

It should be noted that unlike Fig. 3 and Fig. 5 in sections 3.1 and 3.2 respectively that had the same x-axis scale throughout the figures while showing different property of the same materials, figures in this section have different x-axis scale as the comparison between three different materials were made.

Once the shifting factor, a_T, were defined for each aging temperatures, it was possible to access the activation energy (E_a) as described in Eq. 1 for each material, as shown in Fig. 9 and Table 1.

In Arrhenius approach, the activation energy is defined as the energy required to reach the transition state. In case of our study, hydrolysis was the only degradation mechanism and the stress at break was used as the consequence of this hydrolysis reaction. At this stage two main conclusions can be made – (1) that all materials undergo hydrolysis with the same consequence of losing mechanical strength and becoming brittle, and (2) that all the materials require different activation energy for hydrolysis to take place, with PBSAT being the most sensitive followed by PBSA and PA.

Based on the results and the aforementioned conclusion, it was thus possible to extrapolate the model to predict the materials behaviour of all three materials at a lower temperature.

4.2. Prediction of the stress at break induced by hydrolysis reaction

Following Arrhenius approach, the stress can be defined as described in Eq. 2,

$$\sigma = \sigma_0 e^{-A a_T} \tag{2}$$

where σ is the stress at break after aging at defined time and temperature, σ_0 is the stress at break of the unaged material, A is a constant, and a_T is the shifting factor.

Knowing the a_T coefficient and initial stress at break of unaged material which can be found in Table 1 for each material, it was possible to predict the stress at break depending on time and temperature using the Eq. 2.

To validate the prediction and verify that this is an appropriate model, the prediction was first performed on the same temperature as the experimental results, as shown in Fig. 10.

While the initial aging experimental values represented as symbols in Fig. 10 shows some deviation from the predicted trend depicted as dotted lines up to about 10 h, the decline in the experimental average stress at break coincides well with the predicted trend, showing that the prediction is in line with what has occurred in the aging. This validated the model, showing that it was an appropriate tool to predict the behaviour of the material at other temperatures.

Fig. 10 shows the prediction of material behaviours at lower temperatures. The water temperature at which fishing gears could be lost varies dependent on the location and depth of the ocean. A prediction for lower temperatures ranging from 2 °C to 30 °C, which is the average temperature of Barents Sea and tropical seas such as Caribbean Sea respectively, was made to ensure validity of this model across the global oceans.

With the predictions presented in Fig. 10, the impact of the temperature on the time to stress at break could be observed for all three materials. At 2 °C, the material would persist much longer than at 30 °C. The difference between the three materials can also be seen in Fig. 10. However, comparison across each material was a challenging task given the differences in initial strength. Instead of comparing the absolute strength in MPa, a comparison of normalized stress as a percentage to the initial strength and prediction at 15 °C was done in Fig. 11.

With this prediction, it was possible to observe that PBSAT would lose more than a third of its strength already within the first year of complete submersion in water, while PBSA would lose about 10 %, and PA would barely have any change. Within 10 years under water, PBSAT would have lost >95 % of its original strength, while PBSA would have lost approximately 70 % of the strength at 15 °C. Based on the predictions made, PA would only lose approximately 5 % of its initial strength after a decade. A more rapid decline was seen between 10 and 100, and 100 and 1000 years for PBSA and PA respectively. This result is in agreement with the nets removed after approximately 30–40 years of immersion in the ocean, which were not brittle, even if they were subjected to a much more severe environment with several degradation paths including but not limited to hydrolysis, UV-oxidation, biodegradation and mechanical wear and tear (Standal et al., 2020). It was also
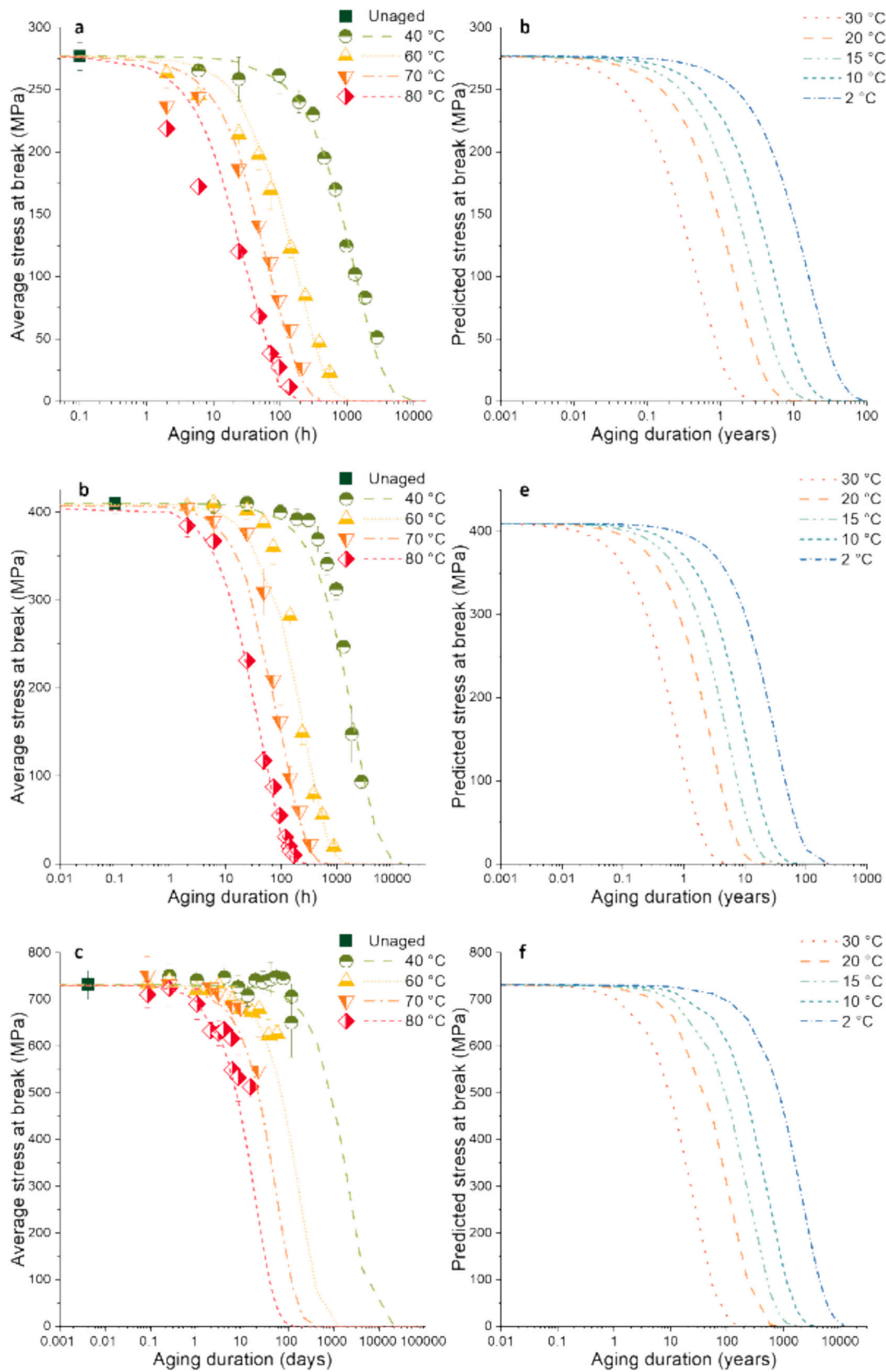
Fig. 10. Stress versus time for (a) PBSAT, (b) PBSA, and (c) PA, at 80 °C (red), 70 °C (orange), 60 °C(yellow) and 40 °C(green). Experimental values in points prediction as dashed lines, and prediction of the stress at break versus time for (d) PBSAT, (e) PBSA, and (f) PA immersed at 2 °C, 10 °C, 15 °C, 20 °C and 30 °C. (For interpretation of the references to colour in this figure legend, the reader is referred to the web version of this article.)
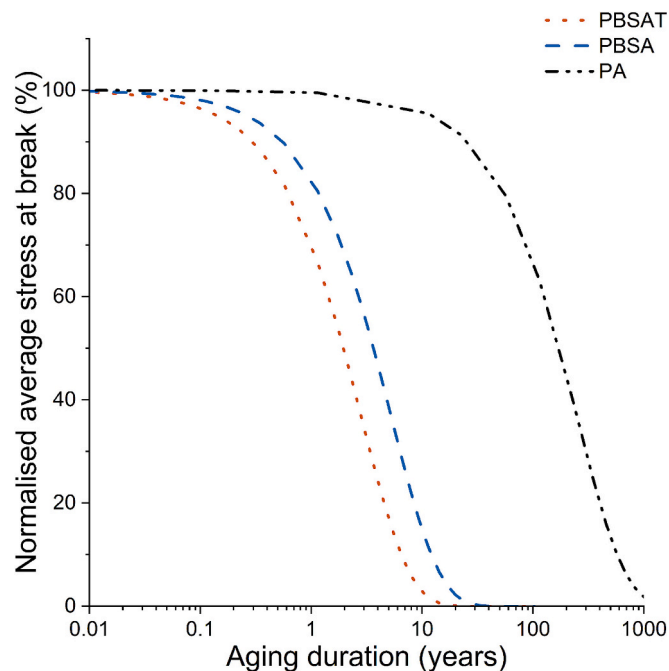
Fig. 11. Normalized stress versus time at 15 °C submersion for PBSAT, PBSA and PA.

reported that lost gears could continuously catch organisms with a relatively constant rate of 20–30 % of the initial efficiency, up to at least 8 years after being lost, and possibly for as long as the material strength remains (Brown et al., 2005; Humborstad and Løkkeborg, 2003).

Since the stress at break could be predicted using the Arrhenius equation in function of the water temperature for the three materials when they would be in abiotic environment, it was possible to set the end-of-life criteria of those materials and predict the time taken to reach such criteria. Determining the end-of-life criteria was highly complicated, as the ability for the organisms to escape from ALDFG depends on various factors including duration of immersion, species, methods of escape, the presence of hard-shell, weight and strength. To our knowledge there is no published work on the force needed by a fish to escape a fishing gear. Consequently, there was no one single value that could be used as a reference point. The end-of-life criteria was therefore hereby specified as 25 %, 50 %, 60 % and 75 % of the initial stress at break of the material.

Fig. 12 shows the time to reach respective end-of-life criteria for each material from 2 °C to 30 °C. Using this figure, an approximate time to reach the specified end-of-life criteria namely between 25 % to 75 % of the stress at break could be predicted. As expected, when temperature increases, the time to reach end-of-life criteria decreases. For PBSAT, PBSA and PA, the longest time needed to reach end-of-life criteria at 2 °C and 25 % of the initial stress at break is slightly >20 years, 40 years and approximately 3000 years respectively. However, 25 % was much probably a too low criterion. Therefore, to compare the materials, a criterion of 50 % had been taken to compare the three materials, as shown in Fig. 12.

Fig. 13 compares the time to reach 50 % of the initial stress at break of PBSAT, PBSA and PA from 2 °C to 30 °C based on the prediction made. It was possible to observe that at 2 °C, which is in the range of the bottom sea temperature, PBSAT, PBSA and PA would reach 50 % of their initial stress at break after approximately 10, 20 and 1500 years respectively. These durations are far longer than the average service time of nets which are usually replaced after one or two seasons, equating to as short as two months of usage. This shows the great potential of PBSAT and PBSA to reduce long-lasting marine littering and mitigate problems deriving from ALDFG. This prediction from this study also demonstrates

the "over-efficiency" of the PA for the application (Grimaldo et al., 2020).

In March 2024, a net piece shown in Fig. 14a made of PA-6 (Kapron) was captured during a bottom trawl experiment at 250 m depth at Nordkappbanken (71°16′ N - 26°45′ E), western part of the Barents Sea. The net was labelled "2.4.79″ as shown in Fig. 14b, with an inscription in Russian translated to "lower net". Due to a regulation change, nets with mesh size 125 mm in bottom trawls were no longer legal after 1983. Based on the available information, it could be deduced that this net was in use between 1979 and 1983 and must have been submerged for more than four decades to date. It was found that these nets were still very strong. While the material may not be identical, and although the braided multifilaments could not be compared directly to multifilaments used in todays' gear, it is of no doubt that polymer in the PA family could persist in the ocean for a long time, especially at low temperatures and none or very low light exposure. However, Thomas and Hridayanathan (2006) have demonstrated unequivocally that PA fishing net materials are highly prone to degradation when exposed to sunlight. Multifilament material is indisputably more vulnerable than monofilament, suggesting that monofilaments in the PA family could persist in the same environment for an even longer time (Thomas and Hridayanathan, 2006). This strength of PA material and the resistance to degradation despite a long submersion time corresponds to our prediction.

4.3. Limit of the prediction

In our beliefs, the results and the prediction presented in this paper allow a comparison of biodegradable material with conventional material for fishing gear application and a greater understanding of the degradation pathways of the biodegradable materials. However, this prediction has several limitations that could be further discussed and developed.

This prediction considered only one chemical degradation process namely pure hydrolysis. However, in the natural environment, a lot of other degradation mechanisms could be concomitant such as other chemical degradation from photo-oxidation or biodegradation from microorganisms, or physical degradation through waves action, and abrasions (Lucas et al., 2008; Rhodes, 2018).

The degradation pathway that ALDFG would be subjected to is highly dependent on where the ALDFG are found. For example, photo-oxidation induced by UV only happen on the surface and on the first layer of the sea where light could penetrate sufficiently strong, whereas hydrolysis occurs everywhere in the ocean due to the presence of water. For this reason, this study had decided to investigate pure hydrolysis as this degradation mechanism will happen, regardless of the geographical position of the ALDFG in the ocean or locality of ALDFG in the water column. Even if the gears would move through the water or along the seafloor, experiencing changes in the immediate environment such as a change in temperature or presence of different microorganisms, hydrolysis will still occur.

A much shorter time, up to a hundred-fold, would be required to reach the defined end-of-life criteria in biodegradable PBSAT and PBSA than conventional PA as seen in section 4.2. For this reason, ALDFG that are manufactured from biodegradable PBSAT and PBSA are likely to lose its strength more quickly, and in turn would be less detrimental in terms of ghost fishing capability. It is also important to note that this study was conducted on monofilaments, rather than fishing nets which undergo heat-treatment during production to spread mesh size evenly and strengthen the knots (Kim et al., 2020). A study as early as 1973 indicated that the presence of knot reduces the effective strength of the fishing net (Radhalekshmy and Gopalan Nayar, 1973). A more recent study by Le Gué et al. in 2024 also indicated that knots contribute to a reduction of half the stress at break of unaged material (Le Gué et al., 2024). The actual time to end-of-life for nets and gears are therefore expected to be shorter than predicted time in this study in terms of the number of years than what is currently presented, as this study only
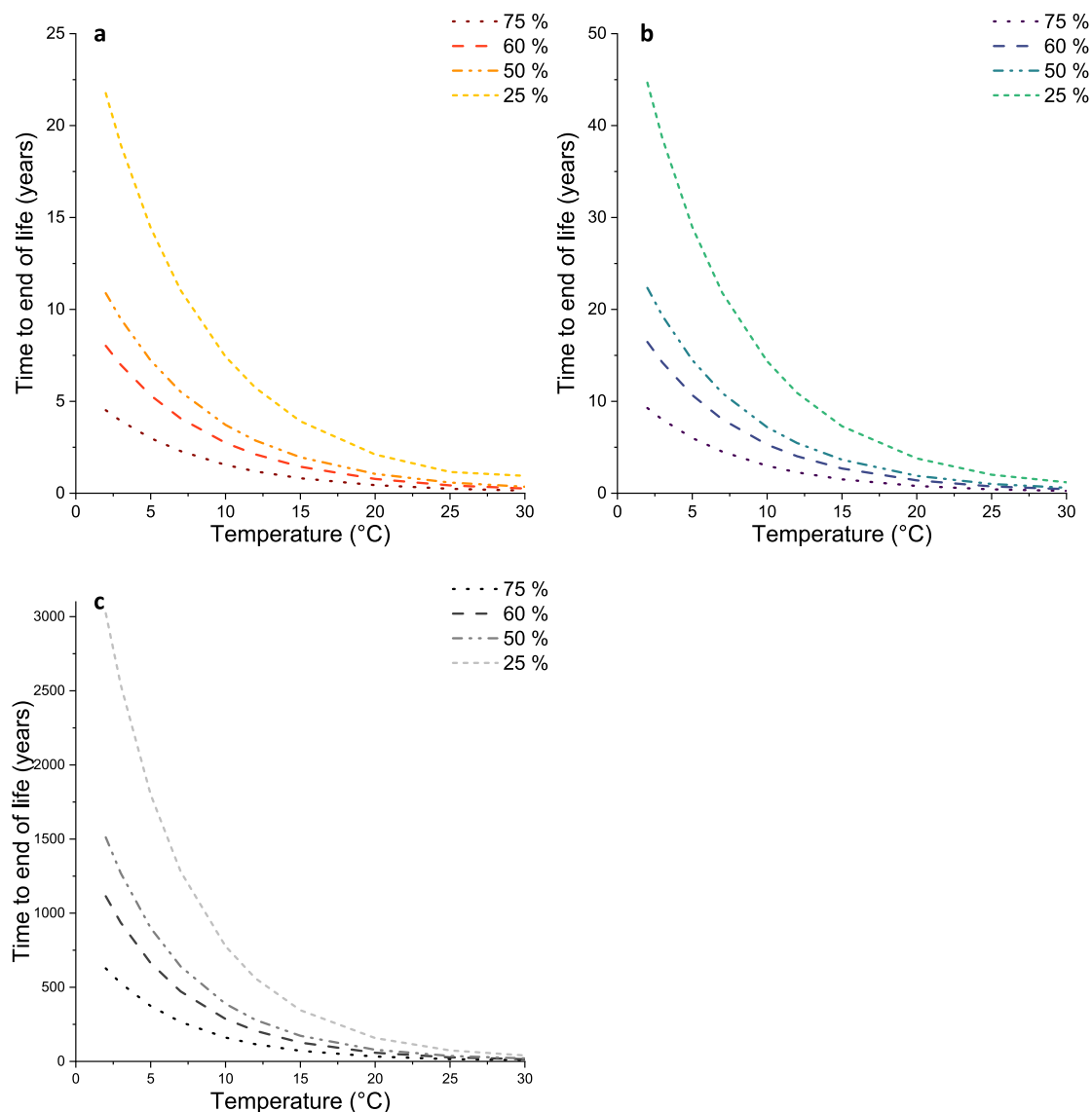
Fig. 12. Time to end-of-life in function of the temperature for different end-of-life criteria taken as 75 %, 60 %, 50 % and 25 % of initial stress at break for (a) PBSAT, (b) PBSA, and (c) PA.

examined monofilaments. The weakening of strength due to both knot forming and heat treatment were not taken into account in this study.

While various studies and reports have addressed the estimated catch and ghost fishing impact of ALDFG and proposed mitigation strategies, fewer studies have explored the use of biodegradable materials as a targeted solution. Biodegradable materials, which have a shorter lifespan compared to PA, are specifically investigated to reduce ghost fishing by considering the changes in their mechanical properties over time. For instance, Araya-Schmidt and Queirolo (2019) analysed the breaking strength of natural fibre twines as a potential alternative to conventional fishing gear for mitigating ghost fishing twines (Araya-Schmidt and Queirolo, 2019). However, their study did not include a comparison with non-biodegradable twines. Similarly, a 2016 study by Kim et al. examined the physical properties of nylon compared to biodegradable PBS/PBAT monofilaments and nets. SEM images revealed signs of biodegradation in PBS/PBAT after 24 months, suggesting that the net would lose its fishing capability. However, the study provided no data on the mechanical properties of the net at this two-year mark (Kim et al., 2016). Several other studies have evaluated changes in mechanical properties, such as elasticity and tensile strength, to assess the differences in fishing efficiency between biodegradable and PA-based

fishing gears. These studies concluded that biodegradable fishing gears could reduce ghost fishing primarily due to their weaker initial strength and limited durability, rather than a gradual reduction in tensile strength over time (Grimaldo et al., 2019; Grimaldo et al., 2018a; Grimaldo et al., 2018b). Brakstad et al. (2022) characterized the degradation mechanisms of PBSAT and PA nets over 36 months in seawater. They demonstrated a significant reduction in mechanical strength for PBSAT nets, while PA nets showed negligible changes. The authors concluded that PBSAT nets could effectively reduce ghost fishing (Brakstad et al., 2022). Additionally, biodegradable fishing gear is sometimes proposed as a solution primarily focused on reducing macro- and microplastic pollution rather than directly addressing ghost fishing (Le Gué et al., 2023).

5. Conclusions

PBSAT and PBAT are *co*-polyester materials manufactured from fossil-fuel based sources developed as a potential material for fishing gears in place of PA. Since fishing gears such as gillnets could be replaced as early as two months in some fisheries, it is unnecessary for them to be manufactured from such a durable material in contrast to the
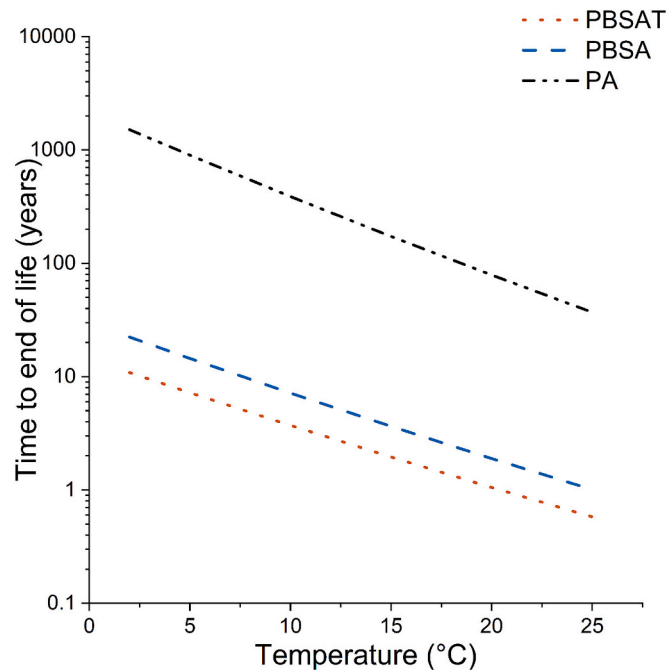
Fig. 13. Time to end-of-life in function of the temperature for end-of-life criteria defined at 50 % initial stress at break.

past where nets had to be mended and used for as long as possible. PBSAT and PBSA are biodegradable materials, with a lower durability and thus a shorter lifespan than PA. Being biodegradable could mean that if fishing gears that are made from PBSAT and PBSA become ALDFG, over time, a full biodegradation into substance harmless to the environment of these materials would be possible. However, biodegradation varies between different geographic conditions, depths and associated environmental conditions depending on for instance what microorganisms are present in the location. Nevertheless, what holds true for all ALDFG in the open ocean when submerged is that hydrolysis aging will definitely occur, no matter the locality, depth or temperatures. This study has shown that PBSAT and PBSA which are co-polyesters, become completely brittle with pure hydrolysis within days at 60 °C, 70 °C and 80 °C. *Co*-polyester bonds are known to be more susceptible to hydrolysis in comparison with polyamide bonds. While these temperatures may not reflect the true environmental conditions, a prediction model based on Arrhenius equation was possible as this was a single factor aging. From the prediction at 15 °C, PBSAT and PBSA would lose almost all its strength after about 10 and 50 years respectively, in comparison to >1000 years for PA. This meant that even in the

absence of other factors and in an abiotic environment, PBSAT and PBSA would be degraded after a relatively much shorter time than PA only through hydrolysis process. Monofilaments, prior to being knotted and heat treated into fishing nets, are known to have higher mechanical strength than nets with knots, as breakage predominantly occurs at the knots. Therefore, the predicted time to end-of-life for nets through pure hydrolysis is likely to be shorter than as shown in this study due to the presence of knots. The aging may also be accelerated in environmental conditions with other additional factors such as wave actions and biodegradation in the presence of microorganisms. Similar studies could be carried out with nets to investigate if the degradation through hydrolysis follow the same trend. A comparison to study aging of fishing net would also be complementary to this result. Further information on the strength of the fish could also contribute positively to evaluate the extent of ghost fishing based on the tensile strength of the material. It would also be interesting to further investigate the influence of the other degradation mechanisms depending on the position or seasons of the year. It is recommended that future research include additional long-term degradation experiments, accompanied by subsequent analyses conducted in the context of field trials and under the actual conditions of
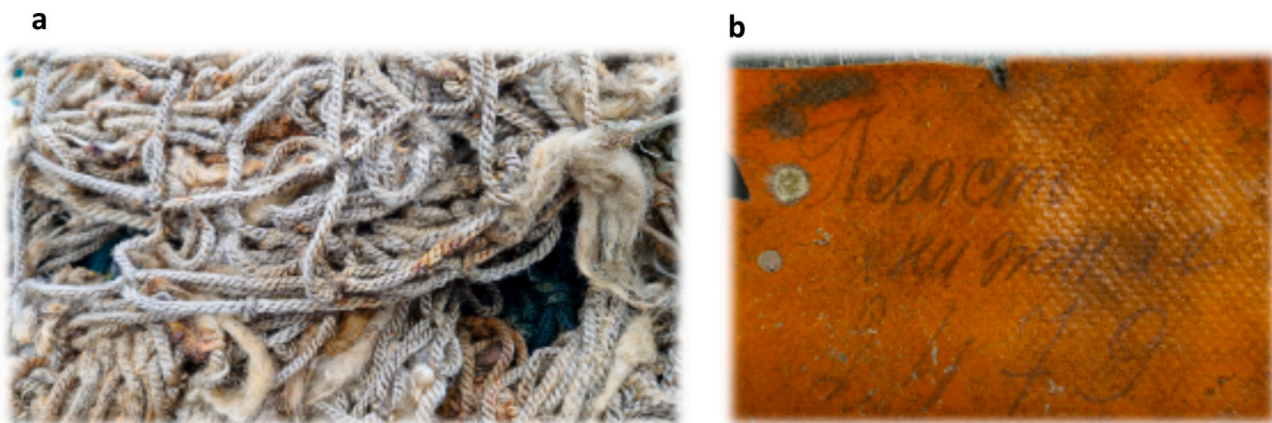
a

b

Fig. 14. (a) PA-6 net with braided monofilaments and mesh size 125 mm and (b) attached net label. Photo*s* by R.B. Larsen, UiT The Arctic University of Norway.

utilisation of the fishing nets as they are deployed in the field. Similar experiment at lower temperature could also be done to confirm the predictions done by this study. Given the duration predicted for biodegradable PBSAT and PBSA to become completely brittle and thus no longer have the ability to ghostfish, the questions with regards to other problems such as microplastics and chemical leaching still remained. It would also be important to study the end product, biodegradation profile and the potential leaching of chemicals of these biodegradable materials. Through this study, it was demonstrated that solely through only exposure to pure water, the differences between the time taken to lose of strength in PA and biodegradable materials could be up to more than a hundred folds, depending on the temperature. This result clearly demonstrates that for a short application time, the use of such resistant material like PA may not be necessary for instance in gillnets fisheries.

CRediT authorship contribution statement

Waranya Wataniyakun: Writing – original draft, Visualization, Methodology, Investigation, Formal analysis, Conceptualization, Writing – review & editing. **Maelenn Le Gall:** Writing – original draft, Visualization, Supervision, Resources, Methodology, Formal analysis, Conceptualization, Writing – review & editing. **Maria El Rakwe:** Writing – original draft, Resources, Writing – review & editing. **Christian W. Karl:** Writing – original draft, Supervision, Writing – review & editing. **Roger B Larsen:** Writing – original draft, Supervision, Resources, Writing – review & editing.

Declaration of competing interest

The authors declare that they have no known competing financial interests or personal relationships that could influence the work reported in this paper.

Acknowledgements

Appendix A. Supplementary data

Supplementary data to this article can be found online at https://doi.org/10.1016/j.marpolbul.2025.117607.

Data availability

Data will be made available on request.

References

Araya-Schmidt, T., Queirolo, D., 2019. Breaking strength evaluation of biodegradable twines to reduce ghost fishing in the pot and trap fisheries of Chile. Lat. Am. J. Aquat. Res. 47 (1), 201–205. https://doi.org/10.3856/vol47-issue1-fulltext-24.

Barnes, D.K.A., Galgani, F., Thompson, R.C., Barlaz, M., 2009. Accumulation and fragmentation of plastic debris in global environments. Philos. Trans. R. Soc. B 364 (1526), 1985–1998. https://doi.org/10.1098/rstb.2008.0205.

Bergmann, M., Collard, F., Joan, F., Gabrielsen, G.W., Provencer, J.F., Rochman, C.M.R., van Sebille, E., Tekman, M.B., 2022. Plastic pollution in the Arctic. Nature Reviews Earth & Environment. https://doi.org/10.1038/s43017-022-00279-8.

Brakstad, O. G., Lisbet, S., Hakvåg, S., Heidi, M. F., Su, B., Aas, M., Ribicic, D., & Grimaldo, E. (2022). The fate of conventional and potentially degradable gillnets in a seawater-sediment system. 180(February). doi:https://doi.org/10.1016/j.marpolbul.2022.113759.

Brown, J., Macfadyen, G., Huntington, T., Magnus, J., Tumilty, J., 2005. Ghost Fishing by Lost Fishing Gear.

Deshpande, P.C., Philis, G., Brattebø, H., Fet, A.M., 2020. Using material flow analysis (MFA) to generate the evidence on plastic waste management from commercial fishing gears in Norway. Resour. Conserv. Recycl. X, 5(February 2019), 100024. https://doi.org/10.1016/j.rcrx.2019.100024.

Fauser, P., Vorkamp, K., Strand, J., 2022. Residual additives in marine microplastics and their risk assessment – a critical review. Mar. Pollut. Bull. 177 (October 2021), 113467. https://doi.org/10.1016/j.marpolbul.2022.113467.

Galgani, F., Hanke, G., Maes, T., 2015. Global distribution, composition and abundance of marine litter. In: Bergmann, M., Gutow, L., Klages, M. (Eds.), Marine Anthropogenic Litter. Springer International Publishing, pp. 29–56. https://doi.org/10.1007/978-3-319-16510-3_2.

Gewert, B., Plassmann, M.M., Macleod, M., 2015. Pathways for degradation of plastic polymers floating in the marine environment. Environ Sci Process Impacts 17, 1513–1521. https://doi.org/10.1039/c5em00207a.

Geyer, R., Jambeck, J.R., Law, K.L., 2017. Production, use, and fate of all plastics ever made. Sci. Adv. 3 (7), 25–29. https://doi.org/10.1126/sciadv.1700782.

Gilman, E. L., Ecosystems, P., Chopin, F., Suuronen, P., & Kuemlangan, B. (2016). *Abandoned, lost and discarded gillnets and trammel nets Methods to estimate ghost fishing mortality, and the status of regional* (Issue January).

Good, T.P., June, J.A., Etnier, M.A., Broadhurst, G., 2010. Derelict fishing nets in Puget Sound and the Northwest Straits : patterns and threats to marine fauna. Mar. Pollut. Bull. 60 (1), 39–50. https://doi.org/10.1016/j.marpolbul.2009.09.005.

Grimaldo, E., Herrmann, B., Jacques, N., Kubowicz, S., Cerbule, K., Su, B., & Larsen, R. (2020). The effect of long-term use on the catch efficiency of biodegradable gillnets. 161(November). doi:https://doi.org/10.1016/j.marpolbul.2020.111823.

Grimaldo, E., Herrmann, B., Su, B., Føre, H.M., Vollstad, J., Olsen, L., Larsen, R.B., Tatone, I., 2019. Comparison of fishing efficiency between biodegradable gillnets and conventional nylon gillnets. Fish. Res. 213 (January), 67–74. https://doi.org/10.1016/j.fishres.2019.01.003.

Grimaldo, E., Herrmann, B., Tveit, G.M., Vollstad, J., Schei, M., 2018a. Effect of using biodegradable gill nets on the catch efficiency of Greenland halibut. Marine and Coastal Fisheries 10 (6), 619–629. https://doi.org/10.1002/mcf2.10058.

Grimaldo, E., Herrmann, B., Vollstad, J., Su, B., Moe Føre, H., Larsen, R.B., Tatone, I., Pol, M., 2018b. Fishing efficiency of biodegradable PBSAT gillnets and conventional nylon gillnets used in Norwegian cod (Gadus morhua) and saithe (Pollachius virens) fisheries. ICES J. Mar. Sci. 75 (6), 2245–2256. https://doi.org/10.1093/icesjms/fsy108.

Grimaldo, E., Karl, C.W., Alvestad, A., Persson, A.M., Kubowicz, S., Olafsen, K., Hatlebrekke, H.H., Lilleng, G., Brinkhof, I., 2023. Reducing plastic pollution caused by demersal fisheries. Mar. Pollut. Bull. 196 (October), 115634. https://doi.org/10.1016/j.marpolbul.2023.115634.

Hahladakis, J. N., Velis, C. A., Weber, R., Iacovidou, E., & Purnell, P. (2018). An overview of chemical additives present in plastics : Migration, release, fate and environmental impact during their use, disposal and recycling. J. Hazard. Mater., 344, 179–199. doi:https://doi.org/10.1016/j.jhazmat.2017.10.014.

Hammer, J., Kraak, M.H.S., Parsons, J.R., 2012. Plastics in the marine environment: The dark side of a modern gift. In: Whitacre, D.M. (Ed.), Reviews of Environmental Contamination and Toxicology. Springer, New York, pp. 1–44.

Hermabessiere, L., Dehaut, A., Paul-Pont, I., Lacroix, C., Jezequel, R., Soudant, P., Duflos, G., 2017. Occurrence and effects of plastic additives on marine environments and organisms: a review. Chemosphere 182, 781–793. https://doi.org/10.1016/j.chemosphere.2017.05.096.

Humborstad, O., Løkkeborg, S., 2003. Catches of Greenland halibut. Reinhardtius hippoglossoides (O.F.), 163–170. https://doi.org/10.1016/S0165-7836(03)00215-7 in Deepwater ghost-fishing gillnets on the Norwegian continental slope.

IWC. (2013). Report of the 2013 IWC Scientific Committee workshop on Marine Debris.

Jambeck, J.R., Geyer, R., Wilcox, C., Siegler, T.R., Perryman, M., Andrady, A., Narayan, R., Law, K.L., 2015. Plastic waste inputs from land into the ocean. Science 347 (6223).

Jang, M., Shim, W.J., Cho, Y., Han, G.M., Ha, S.Y., Hong, S.H., 2024. Hazardous chemical additives within marine plastic debris and fishing gear: occurrence and implications. J. Clean. Prod. 442 (November 2023), 141115. https://doi.org/10.1016/j.jclepro.2024.141115.

Kiessling, T., Gutow, L., Thiel, M., 2015. Marine litter as habitat and dispersal vector. In: Bergmann, M., Gutow, L., Klages, M. (Eds.), Marine Anthropogenic Litter. Springer International Publishing, pp. 141–181. https://doi.org/10.1007/978-3-319-16510-3_6.

Kim, S., Kim, P., Jeong, S., Lee, K., Oh, W., 2020. Physical properties of biodegradable fishing net in accordance with heat-treatment conditions for reducing ghost fishing. Turk. J. Fish. Aquat. Sci. 20 (2), 127–135. https://doi.org/10.4194/1303-2712-v20_2_05.

Kim, S., Kim, P., Lim, J., An, H., Suuronen, P., 2016. Use of biodegradable driftnets to prevent ghost fishing: physical properties and fishing performance for yellow croaker. Anim. Conserv. 19 (4), 309–319. https://doi.org/10.1111/acv.12256.

Koelmans, A.A., Bakir, A., Burton, G.A., Janssen, C.R., 2016. Microplastic as a vector for Chemicals in the Aquatic Environment: critical review and model-supported reinterpretation of empirical studies. Environ. Sci. Technol. 50 (7), 3315–3326. https://doi.org/10.1021/acs.est.5b06069.

Krause, S., Molari, M., Gorb, E.V., Gorb, S.N., Kossel, E., Haeckel, M., 2020. Persistence of plastic debris and its colonization by bacterial communities after two decades on the abyssal seafloor. Sci. Rep. 10 (1), 1–15. https://doi.org/10.1038/s41598-020-66361-7.

Laist, D.W., 1987. Overview of the biological effects of lost and discarded plastic debris in the marine. Environment 18 (June).

Laist, D.W., 1997. Impacts of Marine Debris : Entanglement of Marine Life in Marine Debris Including a Comprehensive List of Species with Entanglement and IngestiOn Records. https://doi.org/10.1007/978-1-4613-8486-1.

Le Gué, L., Davies, P., Arhant, M., Vincent, B., Tanguy, E., 2023. Mitigating plastic pollution at sea: natural seawater degradation of a sustainable PBS/PBAT marine rope. Mar. Pollut. Bull. 193. https://doi.org/10.1016/j.marpolbul.2023.115216.

Le Gué, L., Savina, E., Arhant, M., Davies, P., Gayet, N., Vincent, B., 2024. Degradation mechanisms in PBSAT nets immersed in seawater. Polym. Degrad. Stab. 225 (March). https://doi.org/10.1016/j.polymdegradstab.2024.110788.

Link, J., Segal, B., & Miguel, L. (2019). Abandoned, lost or otherwise discarded fishing gear in Brazil : A review. Perspectives in Ecology and Conservation, 17(1), 1–8. doi: https://doi.org/10.1016/j.pecon.2018.12.003.

Lucas, N., Bienaime, C., Belloy, C., Queneudec, M., Silvestre, F., Nava-saucedo, J., 2008. Chemosphere Polymer biodegradation : Mechanisms and estimation techniques. 73, 429–442. https://doi.org/10.1016/j.chemosphere.2008.06.064.

Lusher, A., Hollman, P., Mendoza-Hill, J., 2017. Microplastics in fisheries and aquaculture. Food and Agriculture Organization of the United Nations. 9–24. https://openknowledge.fao.org/server/api/core/bitstreams/a9a298e0-9db6-4769-beac-37325be3e280/content.

Macfadyen, G., Huntington, T., & Cappell, R. (2009). Abandoned, lost or otherwise discarded fishing gear.

Min, K., Cuiffi, J.D., Mathers, R.T., 2020. Ranking environmental degradation trends of plastic marine debris based on physical properties and molecular structure. Nature. Communications 11 (1). https://doi.org/10.1038/s41467-020-14538-z.

Morales-caselles, C., Viejo, J., Martí, E., González-fernández, D., Pragnell-raasch, H., González-gordillo, J.I., Montero, E., Arroyo, G.M., Hanke, G., Salvo, V.S., Basurko, O. C., Mallos, N., Lebreton, L., Echevarría, F., Emmerik, T., Van Duarte, C.M., Gálvez, J. A., Sebille, E., Van Galgani, F., Cózar, A., 2021. An inshore–offshore sorting system revealed from global classification of ocean litter. Nature Sustainability 4 (June). https://doi.org/10.1038/s41893-021-00720-8.

Norwegian Directorate of Fisheries. (2023). Redskapsopprensking. https://www.fiskeridir.no/Areal-og-miljo/Marin-forsoepling/Redskapsopprensking#:~:text=Fisker idirektoratet har siden tidlig på,farligst i forhold til spøkelsesfiske.

Radhalekshmy, S.K., Gopalan Nayar, S., 1973. Synthetic Fibres for fishing gear. Fish. Technol. 10 (2), 142–165.

Rhodes, C.J., 2018. Plastic pollution and potential solutions. Sci. Prog. 101 (3), 207–260. https://doi.org/10.3184/003685018X15294876706211.

Smolowitz, R.J., 1978. Trap design and ghost fishing: discussion. MFR paper 1310. Mar. Fish. Rev. 40 (5–6), 59–67.

Standal, D., Grimaldo, E., Larsen, R.B., 2020. Governance implications for the implementation of biodegradable gillnets in Norway. Mar. Policy 122 (June), 104238. https://doi.org/10.1016/j.marpol.2020.104238.

Summers, J. W., & Rabinovitch, E. B. (1999). Weatherability of vinyl and other plastics. In weathering of plastics testing to Mirror real life performance (pp. 61–68). Doi:doi: https://doi.org/10.1016/B978-188420775-4.50006-4.

Thomas, S.N., Hridayanathan, C., 2006. The effect of natural sunlight on the strength of polyamide 6 multifilament and monofilament fishing net materials. Fish. Res. 81 (2), 326–330. https://doi.org/10.1016/j.fishres.2006.06.012.

Thompson, R.C., Swan, S.H., Moore, C.J., Saal, F.S., Vom Saal, F.S., Saal, F.S., 2009. Our plastic age. Philosophical Transactions of the Royal Society B: Biological Sciences 364 (1526), 1973–1976. https://doi.org/10.1098/rstb.2009.0054.

Vodopia, D., Verones, F., Askham, C., Larsen, R.B., 2024. Retrieval operations of derelict fishing gears give insight on the impact on marine life. Mar. Pollut. Bull. 201 (March). https://doi.org/10.1016/j.marpolbul.2024.116268.

Wang, J., Tan, Z., Peng, J., Qiu, Q., Li, M., 2016. The behaviors of microplastics in the marine environment. Mar. Environ. Res. 113, 7–17. https://doi.org/10.1016/j.marenvres.2015.10.014.

Welden, N.A., Cowie, P.R., 2017. Degradation of common polymer ropes in a sublittoral marine environment. Mar. Pollut. Bull. 118 (1–2), 248–253. https://doi.org/10.1016/j.marpolbul.2017.02.072.

Wilcox, C., Mallos, N.J., Leonard, G.H., Rodriguez, A., Hardesty, B.D., 2016. Using expert elicitation to estimate the impacts of plastic pollution on marine wildlife. Mar. Policy 65, 107–114. https://doi.org/10.1016/j.marpol.2015.10.014.

World Animal Protection International, 2014. Fishing's Phantom Menace (How ghost fishing gear is endangering our sea life).